Global, Long-Term Sulphur Dioxide Measurements From TOVS Data: A New Tool for Studying Explosive Volcanism and Climate

A. J. Prata[1], W. I. Rose[2], S. Self[3], and D. M. O'Brien[1]

A new technique for retrieving sulphur dioxide concentrations from TIROS Operational Vertical Sounder (TOVS) data is described. The retrieval technique relies on absorption of infrared radiation by the anti-symmetric stretch of the sulphur dioxide (SO_2) molecule centred around 7.3 μm. The High-resolution infrared radiation sounder (HIRS/2) is part of the TOVS package and has a channel that covers this absorption region. The HIRS/2 data are global, span almost 24 years, have a sub-satellite spatial resolution of about 18 km and can be used both day and night. The retrieval method is described and its accuracy and sources of error discussed. Case studies for the June 1991 Pinatubo eruptions, for the August 1991 eruptions of Cerro Hudson and for several eruptions of Hekla volcano, are used to illustrate the retrievals and the results are compared with independent SO_2 retrievals from the TOMS instrument. These new SO_2 data provide a potentially valuable tool for studying the climatic effects of explosive eruptions. Because the satellite measurements are global, long-term and can simultaneously provide other climate parameters (e.g. surface temperatures, temperature profiles, humidity profiles, cloudiness, ozone amount and long- and short-wave radiation) they can be used to test and validate volcanically-induced effects in global climate simulations.

1. INTRODUCTION

The global atmospheric budget of sulphur is important to climate [*Seinfeld and Pandis*, 1998]. Knowledge of the SO_2 component in the atmosphere has come from a variety of sources including ground-based, airborne and more recently satellite-based measurements [*Stoiber and Jepsen*, 1973; *Allard et al.*, 1994; *Pyle et al.*, 1996; *Bluth et al.*, 1993; *Bluth et al.*, 1997]. Estimates of the SO_2 budget provide limits on the amount of H_2SO_4 aerosol in the stratosphere [*Hofmann and Rosen*, 1981], which in turn can be used to evaluate the radiative effects on climate [*Kiehl and Briegleb*, 1993; *Mass and Portman*, 1989; *Robock*, 2000]. Stratospheric sulfuric acid aerosol derives principally from SO_2 injected by volcanic eruptions and these aerosols are important in the chemistry of the stratosphere by providing surfaces for chemical reactions. The current estimate of the stratospheric portion of the flux of SO_2 ranges from ~0.3 Tg a^{-1} to ~3 Tg a^{-1}, with a mean of ~1 Tg a^{-1} [*Pyle et al.*, 1996]. Indirect measurements of this flux have been made from the Total Ozone Mapping Spectrometer (TOMS) satellite [*Bluth et al.*, 1997; *Krueger et al.*, 1995], and more recently from the Global Ozone Monitoring Experiment (GOME)—see for example *Eisinger and Burrows* [1998]. *Rose et al.* [2000] have shown the usefulness of combining different satellite measurements of SO_2 to improve estimates of the atmospheric emission of this gas from volcanic eruptions. Given the importance of the stratospheric budget of SO_2 to climate and the sporadic and global nature of vol-

[1]CSIRO Atmospheric Research, Victoria, Australia.
[2]Geological Engineering and Sciences, Michigan Technological University, Houghton, Michigan, USA.
[3]Department of Earth Sciences, The Open University, Milton Keynes, United Kingdom.

Volcanism and the Earth's Atmosphere
Geophysical Monograph 139

10.1029/139GM05

canic eruptions, it is useful to have other independent satellite measurements of SO_2. The purpose of our work here is to document a source of satellite SO_2 measurements that complement existing measurements and provide a valuable data-set for intercomparison with TOMS and GOME.

The NOAA series of satellites carry the TIROS Operational Vertical Sounder (TOVS) instrument package which includes the High-resolution Infrared Radiation Sounder (HIRS/2–see *Smith et al.*, [1979]). This instrument measures infrared radiation in nineteen narrow channels (bandwidths ≈0.5–1 μm) with the purpose of retrieving atmospheric temperature and moisture profiles. One channel (channel 11) completely covers the strong, anti-symmetric stretch vibration (v_3-band) of SO_2 situated near 7.34 μm (see Figure 1). This channel is used for tropospheric water vapour sounding, but it is shown here that provided the water vapour lies below the SO_2, the channel can also be used to measure SO_2 column abundance.

Figure 1 shows the vertical transmittance, in the wavelength range 6–13 μm, for a cloud layer containing 100 m atm-cm (dashed line) and 1000 m atm-cm (solid line) of SO_2, with a width of 2 km, placed at 25 km in an otherwise absorber-free atmosphere.

The main absorption features are the v_1 and v_3 bands, centred near 8.55 μm and 7.34 μm, respectively. Both of these bands can be used to retrieve SO_2 column amounts.[1] The v_1 feature looks particularly interesting because it lies within the 'window' where absorption due to water vapour is smaller. Indeed *Realmuto et al.*, [1994] and *Realmuto* [1996] have developed methods for retrieving SO_2 using this feature from airborne and spaceborne sensors (e.g. MASTER, ASTER and MODIS). Ground-based interferometric measurements have also been made using this band

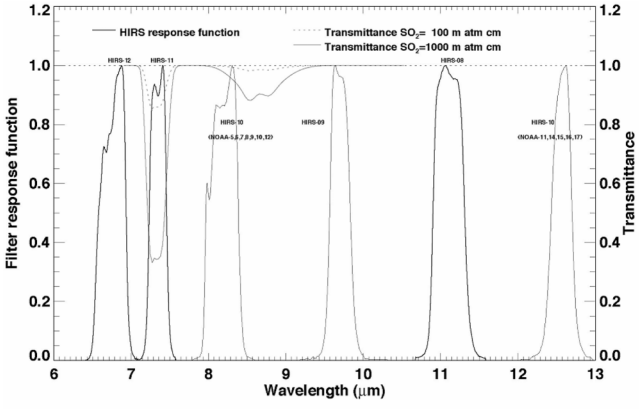

Figure 1. Positions of HIRS/2 filter functions and vertical atmospheric transmittance (100 m atm-cm and 1000 m atm-cm) for the v_1 and v_3 SO_2 bands.

[*Francis et al.*, 1995; *Love et al.*, 1998; *McGee and Gerlach*, 1998]. Use of the v_3-band can be traced to work first published by *Mankin et al.* [1992] and *Goldman et al.* [1992] who used a high spectral resolution instrument (an interferometer) to exploit the 'micro-windows' around 7.3 μm. *Crisp* [1995] was first to suggest that the 7.3 μm band on MODIS could be used to provide an SO_2 alert, but she did not develop a quantitative retrieval procedure. *Ackerman and Strabala* [1994] used HIRS/2 data to study H_2SO_4 aerosols by utilising information in the 8- to 12-μm region. *Baran and Foot* [1994] demonstrated the use of HIRS/2 data and radiative transfer modelling to derive quantitative estimates of H_2SO_4 aerosols. Our work is the first to attempt a quantitative retrieval based on broadband (bandwidths >~0.4 μm) infrared measurements of the v_3 absorption feature of SO_2. In essence the retrieval from satellite-based broadband measurements is possible whenever the SO_2 is well-separated from H_2O and above it. Thus the method is ideally suited to studies of SO_2 that affect the climate, that is, quantitative studies of large volcanic emissions of SO_2 that have been injected into the upper troposphere/lower stratosphere.

In this paper we describe the principle of the retrieval method and suggest a model and methodology for use with HIRS/2 data. Next we discuss the practical implementation of the algorithm and provide a thorough error analysis. Examples of retrievals for several well-studied eruptions are given together with results for the 1996 Mt Ruapehu eruptions–for which no TOMS data were available. Two appendices are provided—Appendix 1 contains a list of the acronyms used throughput the paper, and Appendix 2 contains some of the mathematical detail. Finally, we suggest ways these new data can be used to study the atmospheric effects of explosive volcanism on climate.

2. SO_2 RETRIEVAL FROM INFRARED MEASUREMENTS

2.1 The HIRS/2 Instrument

The first TOVS package was launched on board the TIROS-N satellite in 1978 and the latest is on the NOAA-17 platform-providing 24 years of continuous global measurements. The HIRS/2 instrument includes measurements in 20 channels (19 in the infrared and 1 visible channel)—giving estimates of surface temperature, atmospheric profiles of temperature and moisture, cloudiness and column ozone abundance. These data are used operationally to provide meteorological data for numerical weather forecasting.

Table 1. Characteristics of the HIRS/2 channels relevant to SO_2 retrieval

Channel No.	Central wavelength (μm)	Half-power bandwidth (μm)	Purpose	Weighting function peak (hPa); (km in brackets)
8	11.11	0.45	Surface/clouds	Surface (0–2 km)
9	9.71	0.48	Ozone	25 (25–35 km)
10	8.16/12.47[a]	0.42/0.46[b]	Surface/cloud	900 (1–2 km)
11	7.33	0.44	Water vapour	700 (3–4 km)
12	6.72/6.52[a]	0.37/0.37[b]	Water vapour	500 (5–6 km)

[a] New central wavelength on HIRS/3.
[b] New half-power bandwidth on HIRS/3.

The channels were chosen to maximize information retrieved from radiances sampling different vertical layers of the atmosphere several kilometres thick. Most of the channels lie near strong absorption features (e.g. near to CO_2 or H_2O absorption features), while some channels are located in atmospheric window regions where information about the surface and lower atmosphere can be retrieved. Table 1 provides information about the channels of relevance to this study. Table 2 provides information on the HIRS/2 instrument—more comprehensive information may be found in *Smith et al.* [1979], *Planet* [1988], and *Kidwell* [1991].

The filter functions of the HIRS/2 instrument are also shown in Figure 1, together with SO_2 transmittance of the v_1 and v_3 SO_2 bands. Only the channels at 6.7, 7.3, 8.2, 9.7, 11 and 12 μm are shown—the channels used in the retrieval are plotted using thick lines. Note that the SO_2 v_3 feature is almost entirely covered by HIRS/2 channel 11, while only a small part of the SO_2 v_1 band is covered by channel 10. The HIRS/2 instrument has undergone some changes over its 24 year history; there are in fact three versions of the instrument—HIRS (originally flown on Nimbus-6), HIRS/2 (NOAA-satellite series) and the present HIRS/3. Table 3 provides a chronology of the instruments' service record, spacecraft, launch date, and the node crossing times.

2.2 Transmittance Model

To exploit the SO_2 information contained in the HIRS/2 measurements we employ an accurate transmittance model that relates the absorption in HIRS/2 channel 11 to SO_2 absorber amount. The anti-symmetric stretch of the SO_2 molecule is situated around 7.34 μm and the transmittance of this feature has been modelled using a double-exponential model by *Pierluissi and Tomiyama* [1980] and *Pierluissi et al.* [1984]. We validated this model against line-by-line calculations and found the results to be accurate below about 200 m atm-cm$^{(2)}$. Above this value the model diverged from the line-by-line results. Based on this assessment we decided to use an exponential sum-fitting procedure (ESFT, see *Wiscombe and Evans* [1977]) to the band transmittance. The ESFT model has the form,

$$t_s = \sum_{i=1}^{n} a_i \exp(-k_i u), \tag{1}$$

where t_s is the transmittance (see Appendix 2 for a definition), u is absorber amount, and a_i, k_i are coefficients. This model is accurate over a wide range of absorber amounts and is very fast for use operationally because a table of coefficients can be generated off-line for each assumed absorber layer (characterized by its atmospheric layer pressure and temperature) and for all the satellite filter response functions. Since HIRS/2 channel 11 has a finite bandpass, the coefficients for the band model account for the variation of the absorption across the channel 11 filter function. In practice the absorber amounts are pre-computed for 26 different atmospheric layers, and each HIRS/2 channel 11 on each satellite, in 0.001 transmittance steps. This provides a large look-up table which can be efficiently searched to provide excellent processing

Table 2. Characteristics of the HIRS/2 instruments.

Parameter	Value
Field-of-view	21.8 mrad
Ground field-of-view	
Nadir	18.5 km circular
End of scan	31.8 km × 62.8 km
Scan line	
Scan time	6.4 s
Scan angle	±49.5°
Swath width	±1115 km
Number of spots per scan line	56
Distance between spots	
Cross-track	26.4 km
Along-track	41.8 km
Gap between consecutive passes at the equator	540 km

Table 3. Chronology of the NOAA meteorological satellite series.

Space-craft	Launch date	Ascending node	Descending node	Service period
TIROS-N	Oct-13-1978	15:00	03:00	Oct-19-1978-Jan-30-1980
NOAA-6	Jun-27-1979	19:30	07:30	Jun-27-1979-Nov-16-1986
NOAA-7	Jun-23-1981	14:30	02:30	Aug-24-1981-Jun07-1986
NOAA-8	Mar-28-1983	19:30	07:30	May03-1983-Oct-31-1985
NOAA-9	Dec-12-1984	14:20	02:20	Feb-25-1985-Aug-03-1995
NOAA-10	Sep-17-1986	19:30	07:30	Nov-17-1986-March-1995
NOAA-11	Sep-24-1988	13:30	01:40	Nov-08-1988-Sep-09-1994
NOAA-12	May-14-1991	19:30	07:30	May-14-1991-present
NOAA-13	Aug-09-1993		Power failure 12 days after launch	
NOAA-14	Dec-300-1994	13:40	01:40	Dec-30-01994-present
NOAA-15	May-13-1998	19:26	07:26	Dec-15-1998-present
NOAA-16	Sep-21-2000	14:00	02:00	Sep-21-2000-present
NOAA-17	Jun-24-2002	22:00	10:00	Jun-24-2002-present

speed for global retrievals. The precise look-up tables used are available from the authors on request.

A simplified radiative transfer model is proposed for deriving SO_2 transmittance from the HIRS/2 temperature measurements. The details of the derivation are given in Appendix 2—the main result is given here. As noted in Appendix 2, Eq. (16) may be written in the form:

$$I - I_a = (1 - t_s)(B_s - I_a), \tag{2}$$

where I is the measured radiance at 7.3 μm, I_a is the radiance at 7.3 μm for an atmosphere free of SO_2, t_s is the SO_2 transmittance and B_s is the Planck radiance for the SO_2 cloud layer at temperature T_S This equation suggests that,

$$\Delta T = \alpha + \beta(1 - t_s). \tag{3}$$

where ΔT is the temperature difference corresponding to the difference between the measured radiance and the SO_2-free radiance, obtained using the inverse Planck function. α and β are parameters to be estimated. From analysis of data and from Modtran [*Berk et al.*, 1989] modelling it has been found that,

$$\alpha \approx -8K,$$
$$\beta \approx -32K.$$

In practice α and β are functions of the atmospheric state and, in particular the temperature of the SO_2 cloud. Since the SO_2 cloud temperature is unknown we have used data and modelling to estimate these parameters, but the algorithm still requires an independent estimate of the height of the SO_2 cloud in order to generate the appropriate look-up table.

3. PRACTICAL CONSIDERATIONS

The simple model presented here permits the evaluation of t_S from a measurement of ΔT. For HIRS/2 data, the evaluation of ΔT is made by estimating I_a through a linear interpolation of a radiance measurement at 6.7 μm (HIRS/2 channel 12) and a radiance measurement at 11.1 μm (HIRS/2 channel 8). The use of the 11.1 μm channel is made in preference to a channel at 8.2 μm because this channel is also affected by SO_2 absorption and so cannot give a reliable estimate of the unperturbed atmospheric state. Thus,

$$\begin{aligned} I_a = I_a^{lin} &= a + b\lambda_{7.3} \\ b &= \frac{B\left[T, \lambda_{6.7}\right] - B\left[T, \lambda_{12}\right]}{\lambda_{6.7} - \lambda_{12}} \\ a &= B\left[T, \lambda_{6.7}\right] - b\lambda_{6.7}. \end{aligned} \tag{4}$$

Here all λ subscripts refer to central wavelengths (in μm). Finally,

$$\Delta I_a^{lin} = B\left[T, \lambda_{7.3}\right] - I_a^{lin}. \tag{5}$$

It should be noted that, in general, $\Delta I_a^{lin} < 0$. The HIRS/2 data processing proceeds on a pixel-by-pixel basis.

3.1 Estimating the Background Radiance

The scheme outlined above relies on an estimate of the background (unperturbed) radiance at 7.3 μm, which has been obtained using a linear interpolation (Eq. 5). The accuracy of the linear interpolation of radiance as a function of wavelength has been gauged by studying large amounts of HIRS/2 data for cases where there are no SO_2 clouds present. In most situations this appears to be accurate (within ±2

K in 95% of cases studied). There is however a notable bias with the interpolated value usually higher than the actual value. In some cases, with no SO_2 present, it was found that the linear interpolation was a poor estimate of the observed radiance. Presumably, this is due to the effects of clouds within the HIRS/2 field-of-view. With just a small addition in complexity, a significant improvement to the scheme was made in the following manner:

(1) Blackbody radiance curves are generated using the observed radiances at 6.7 and 11.1 μm, and 'pseudo' radiances ($I^*(T_{\lambda 1}, \lambda_2)$) are calculated at all three wavelengths:

$$I^*\left(T_{11.1}, 6.7\right) = B\left(T_{11.1}, 6.7\right),$$
$$I^*\left(T_{6.7}, 7.3\right) = B\left(T_{6.7}, 7.3\right),$$
$$I^*\left(T_{11.1}, 7.3\right) = B\left(T_{11.1}, 7.3\right),$$
$$I^*\left(T_{6.7}, 11.1\right) = B\left(T_{6.7}, 11.1\right),$$

The blackbody radiance curves bracket the range of possible observed radiances at 7.3 μm. (See Figure 2.)

(2) An estimate of the observed radiance is obtained from:

$$\hat{I}_a = 0.5\left[I^*\left(T_{6.7}, 7.3\right) + I^*\left(T_{11.1}, 7.3\right)\right].$$

(3) An adjustment to the linearly interpolated 7.3 μm radiance is obtained from:

$$I_a^{adj} = 2.0\left[I^*\left(T_{11.1}, 7.3\right) - I^*\left(T_{6.7}, 7.3\right)\right].$$

(4) If the brightness temperature at 11.1 μm is above a certain threshold (270 K is used), then the 7.3 μm radiance estimate is obtained from the adjusted linearly interpolated value; otherwise the average of the 'pseudo' radiances is used:

$$\hat{I}_{a7.3} = I^{lin} - I_a^{adj} \qquad T_{11.1} > T_{thresh},$$
$$\hat{I}_a = 0.5\left[I^*\left(T_{6.7}, 7.3\right) + I^*\left(T_{11.1}, 7.3\right)\right] \quad \text{otherwise}$$

The scheme attempts to account for the effects of multiple layer clouds within the pixel, whilst also remaining relatively simple to implement. Figure 2 provides a graphical illustration of the interpolation scheme for a pixel containing SO_2.

The difficulty in estimating the background radiance lies in the non-linear temperature response from a pixel of mixed composition (i.e. clear-sky and clouds at multiple levels). Ideally the scheme should be designed to first estimate the fractional coverage of cloud within the pixel, together with an estimate of the clouds' height or radiating temperature. Then, under less restrictive assumptions the radiance at 7.3 μm is estimated from clear and cloud-sky radiances separately and combined by weighting the radiances with the fractional cover estimate. Further accuracy could be gained by employing a radiative transfer model with forward calculations and utilising the full suite of HIRS/2 channels. Such improvements are beyond the scope of this paper, and we readily concede that this retrieval scheme suffers limitations.

3.2 The Effects of the HIRS Filter Function

The HIRS filter functions cover approximately 0.44 μm and the response is not constant across the band. *Pierluisi*

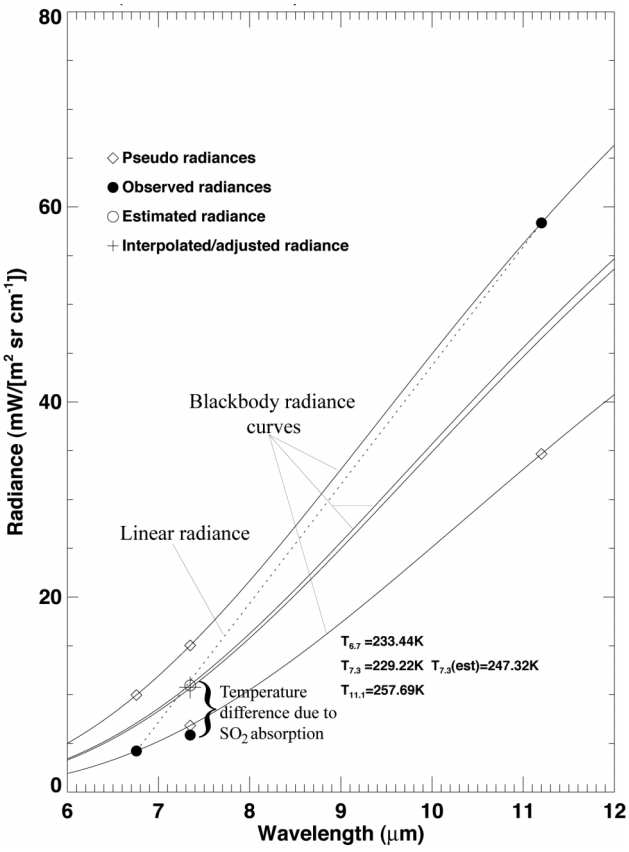

Figure 2. Radiance *vs.* Wavelength for a pixel which contains SO_2. The curves are blackbody radiances at the temperatures found by inverting the Planck function at 6.7 μm and 11.1 μm. The + shows the adjusted linearly interpolated radiance at 7.3 μm, the open circle shows radiance at 7.3 μm derived from Eq. 5, and the solid circles show the measured radiances. The difference between the observed 7.3 μm temperature and the estimated 7.3 μm temperature is the temperature anomaly.

et al. [1984] provide spectral band parameters for SO_2 that can be used to assess the effect of the HIRS filter response on the transmittance. The analysis indicates that the effect is small but important. The difference between assuming a monochromatic transmittance function and doing an integration across the HIRS filter function varies with absorber amount and with the height of the SO_2 cloud. The transmittance difference was found to be less than 0.05 over the whole parameter range and peaked between 10–20 m atm-cm. Above 50 m atm-cm the transmittance difference was less than 0.02. The ESFT scheme employed here accounts for the effects of the HIRS filter functions.

3.3 The Effects of the Surface

The analysis indicates that the surface radiance has only a small effect on the retrieval. This lack of dependence arises through the use of radiances from different channels for the same pixel when estimating the unperturbed radiance at 7.3 μm, and from the fact that this channel is almost opaque, except for very dry atmospheres. For optically thin veils of SO_2[3], the sensitivity of the scheme will prohibit accurate retrievals. A test is used to limit the retrieval to cases where,

$$T_{11.1} < 295K,$$

where $T_{11.1}$ is the (Planck) brightness temperature sensed in the 11.1 μm channel at the top of the atmosphere.

3.4 The Effects of Water Vapour

Residual water vapour absorption may cause anomalies in the retrieval. If there is significant water vapour absorption within the SO_2 cloud then this will also show up as extra absorption in the 6.7 μm channel. This channel is used in the linear interpolation scheme so the algorithm will compensate for the effect of in-cloud water vapour. For cases where there are very high water vapour amounts lying just below the SO_2 cloud it is possible that the retrieval will produce anomalous results. The effect will be worse if the SO_2 cloud is thin—this sets a limit on the lowest SO_2 amount that can be retrieved. There may also be situations where the vertical water vapour distribution causes the linear interpolation scheme to break-down, however these are unlikely to be common situations as they require unusual atmospheric conditions. Finally, SO_2 lying below significant water vapour will not produce a useful signal because the 7.3 μm channel is sensitive to water vapour. This puts a constraint on the lowest level in the atmosphere for which SO_2 can be measured. A rule-of-thumb estimate for this is 3 km, which is the mean water vapour scale height [*Randel et al.*, 1996]. A test is employed to eliminate water vapour anomalies. To pass the test, pixels must satisfy the condition:

$$T_{11.1} > T_{6.7}. \tag{6}$$

Essentially this test regards the brightness temperature in the window channel (11.1 μm) as *always* being *larger* than the brightness temperature in the water vapour channel (6.7 μm). There are occasions when this may not be true (e.g. strong inversions). The test eliminates very few pixels from the retrieval process.

A further test checks that the brightness temperature at 8.2 μm (or 12.5 μm for NOAA-11 and beyond) is larger than the brightness temperature at 11.1 μm, when the 11.1 μm brightness temperature is low (250 K is used). This eliminates some volcanic ash signals and abnormal water vapour and cloud signals. The test is conservative.

3.5 The Effects of Clouds

Water/ice clouds lying above the SO_2 cloud will mask SO_2 absorption and consequently the scheme will not 'see' the SO_2. This can occur for very high, thick (cold) cloud, particularly in the tropics. A test has been devised to limit the retrieval to cases where,

$$T_{11.1} > 200K.$$

This test also doubles to eliminate problems arising from thin SO_2 veils overlying very cold surfaces (e.g. ice covered surfaces in winter), which suffer from the same constraints as described in 3.3.

A second test is employed to remove the effects of poor calibration, pixel misalignment and some abnormal conditions, notably very high water vapour loadings and strong cirrus cloud signals. The test is:

$$T_{8.2} - T_{11.1} < -10K. \tag{7}$$

For satellites after NOAA-10 the test is:

$$T_{12.5} - T_{11.1} < -10K. \tag{8}$$

The thresholds used in these tests were determined through extensive data analysis and trial-and-error. A better approach would be to use an objective cloud detection scheme, such as *English et al.* [1999]. Work is in progress to

include such a scheme. The current tests are preliminary and need refinement.

3.6 Data Integrity Tests

The TOVS data processing is complex and occasionally suspect data are delivered into the processed HIRS/2 data files. There appears to be no systematic problem with the data processing, rather anomalies appear to occur in an unpredictable, almost random manner. To eliminate spurious data a simple spike test has been employed. This takes the form of calculating the mean of 8 neighbouring pixels and testing the pixel being processed against the mean. If the pixel value lies well outside the mean the retrieval halts for this pixel. There is a small cost of losing valid data. That is, having a valid pixel with an anomalously high valid value in the neighbourhood of low values, being eliminated in the process.

3.7 Sensitivity to Cloud Height

The conversion of ΔT measurements into transmittance is relatively straightforward via (3), and the transmittance model (1) allows an estimate of the absorber amount u. However, this conversion has a dependence on pressure and temperature of the absorber (through the pressure and temperature dependence of the ESFT coefficients a_i and k_i); in other words it depends on the location of the SO_2 in the vertical. The dependence on pressure is stronger than that on temperature. Thus, the retrieval requires a height estimate for the SO_2. Figure 3 illustrates the variation of SO_2 absorber amount (u) with temperature anomaly (ΔT) for different cloud heights.

4. ERROR ANALYSIS

Several sources of error have been identified in the retrieval of SO_2 from HIRS/2 infrared measurements. We class these errors into two types: those that contribute to the accuracy of the retrieval and those that limit the operation of the retrieval. The first type of errors (Type I) include as major sources:

- Inherent accuracy of the measurements–the NEΔT,
- Errors in estimating the background radiance,
- Transmittance modelling errors,
- Error in SO_2 cloud height and temperature estimation.

The Noise Equivalent Temperature Difference (NEΔT) of HIRS/2 channels 8, 11 and 12 are ~0.5 K. The background

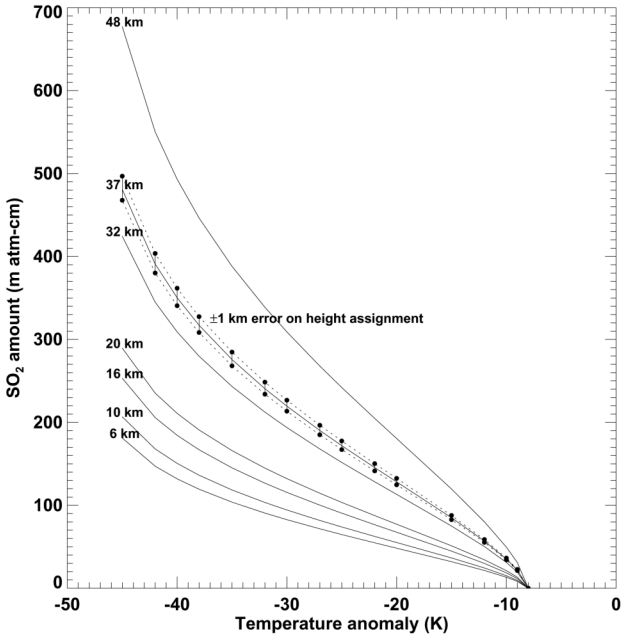

Figure 3. Variation of SO_2 amount with temperature anomaly (ΔT). Each curve shows the variation of the temperature anomaly (ΔT) with absorber amount for a particular SO_2 cloud-top height. An indication of the error resulting from a ±1 km error in the height assignment is also shown.

radiance errors are difficult to estimate theoretically, but can be estimated by analysis of large amounts of HIRS/2 data when no SO_2 clouds are present. These analyses suggest an rms error of ±1 K. Transmittance modelling errors include SO_2 band parameter errors, errors due to misfit in the ESFT procedure, errors in the filter response specification, and errors in the relation between SO_2 transmittance and 7.3 μm temperature differences. The largest of these four sources of error is the latter and we have estimated this to be ±1 K, based on radiative transfer simulations. Combining these errors and assuming that they are independent, the Type I error is:

$$\delta T_i \approx \pm 1.5K.$$

This can be easily assessed by conversion into an error in SO_2 amount by using the sensitivity of the double-exponential model [*Pierluisi et al.*, 1984]. Figure 4 illustrates Type I error in retrieved SO_2 for measurement and modelling errors and two cloud heights.

For relatively low clouds, SO_2 amounts of < 5 D.U. (1 D.U.=1 m atm-cm) are subject to large error and are probably indistinguishable from the noise (unless spatial coherence is evident). For higher clouds this lower thresh-

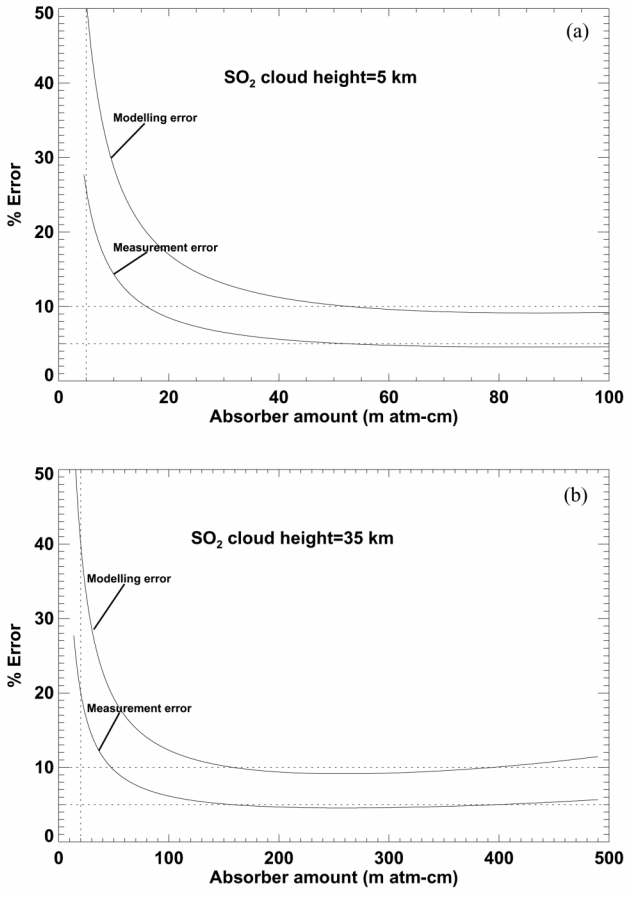

Figure 4. (a) Measurement and modelling errors as a function of absorber amount for a plume at 5 km height and low abundance. (b) Measurement and modelling. errors as a function of absorber amount for a plume at 35 km height and high abundance.

old on the error increases to ~20 D.U. In both cases errors of 5–10% are evident throughout the range of expected absorber amounts. The modelling errors dominate measurement errors—which is encouraging as improvements in the model are possible whilst improving measurement errors are only possible by some form of averaging (e.g. spatial and temporal)

The second type of errors (Type II) include:

- Infrared contrast,
- Model sensitivity,
- Anomalous atmospheric conditions,
- Spectroscopic considerations.

Type II errors are systematic and result from basic violations of the measurement and/or atmospheric assumptions or from lack of knowledge of the physical processes. Because the technique described here involves an infrared atmospheric emission measurement, the ability to retrieve SO_2 relies on the difference in temperature between the emitting source (the SO_2) and the background temperature (due to water vapour or clouds). The lack of 'infrared contrast' fundamentally restricts the technique. Thus if the SO_2 cloud is at the same temperature as the water vapour/cloud/atmosphere below, it is not possible to reliably retrieve the SO_2 amount regardless of its magnitude. Although on average the infrared contrast is adequate, there are persistent conditions where retrieval accuracy is limited. These include geographic locations where the surface below is as cold as the SO_2 cloud itself, for example, over ice-covered Antarctica and Greenland and climatic regions where the SO_2 cloud lies above the tops of high, thick clouds, such as tropical cumulonimbus clouds. Inspection of (2) and (3) shows that $\Delta T \rightarrow 0$, as the infrared contrast decreases $(B_s - I_a)$, regardless of the amount of SO_2 (t_s).

Another drawback of the infrared measurement arises through lack of sensitivity of the model. There are two limiting cases for which SO_2 retrieval is problematic. For very high SO_2 amounts, inspection of (2) shows that as $t_S \rightarrow 0$, the measured radiance arises solely from the SO_2 cloud and consequently the infrared contrast is small. The transmittance model suggests that absorber amounts >~900 D.U. cause saturation. Using the optimal parameters for α and β in (3) with $t_s = 0$, suggests ΔT=–40 K. For very low SO_2 amounts, $t_S \rightarrow 1$ and (3) gives $\Delta T = \alpha$. This case can be investigated further by assuming that values with ΔT below $\alpha - |\delta T_1|$ are at the detection limit. In this case the model gives 3.7 D.U. for a cloud at a height of ~8 km. In practice smaller amounts may be detected by assessing the spatial coherence of the data or by averaging pixels.

Atmospheric conditions for which the basic assumptions of the model are violated include cases where water vapour and/or cloud lies above the SO_2 cloud or when significant water vapour is collocated with the SO_2. Unusual inversions in the temperature and/or water vapour profile may also cause problems with the retrieval. All of these anomalous conditions do occur, but experience with processing the data suggests that they are not common. Perhaps the main area of concern is the occurrence of water vapour coexisting with SO_2 and/or occurring in large enough quantities to cause significant absorption across the 7.3 μm band. This problem is somewhat alleviated because the retrieval scheme makes use of radiance measurements at 6.7 μm, which changes as the mid-tropospheric water vapour changes in a similar fashion to the radiance change at 7.3 μm. Thus the scheme compensates for extra water vapour associated with the SO_2 cloud. Demonstrating unequivocally that water vapour is not a seri-

ous problem will need to wait until routine high spectral resolution data are available across the 7.3 μm band (e.g. from AIRS data–see *Chahine et al.*, [2003]).

5. EXAMPLES

5.1 Pinatubo

Quantitative use of HIRS/2 data to estimate SO_2 has not been made previously and it is therefore necessary to demonstrate what is possible using examples from well-known cases of volcanic SO_2 clouds. One such case is that of the June 1991 Pinatubo eruptions which are generally regarded to have injected ~15–19 Tg of SO_2 into the stratosphere [*Self et al.*, 1996]. Such a large SO_2 anomaly should be readily detectable in the HIRS/2 data.

The Pinatubo SO_2 cloud was measured by the TOMS instrument and also by several other airborne and satellite-borne sensors [*McCormick et al.*, 1995; *Self et al.*, 1996]. During 1991 three HIRS/2 instruments were flying (see Table 2)–on NOAA-10, NOAA-11 and NOAA-12. These satellites had different node crossing times and, since HIRS/2 is an infrared sensor both day and night coverage was possible. Plate 1 shows a time sequence of SO_2 retrievals made from the three HIRS/2 instruments and Table 4 provides a comparison of total masses (determined in the same way as in *Krueger et al.*, 1995, Eq. 15) retrieved from combined HIRS/2 measurements (3 instruments) with TOMS for several days. Generally, the agreement is good: HIRS/2-TOMS=+1.0 Tg, $\sigma = \pm 1.2$ Tg.

5.2 Cerro Hudson

In August 1991, Cerro Hudson erupted sending a large amount (> 1 Tg) of SO_2 into the upper troposphere and lower stratosphere. HIRS/2 retrievals have successfully tracked the SO_2 cloud for nearly 3 weeks as it circled the southern hemisphere at latitudes south of 30 ºS. Plate 2 shows a montage of SO_2 retrievals obtained over a 9-day period as the cloud encircled the hemisphere. Numerical modelling of the cloud transport and TOMS data verify that the cloud passed over southern Australia and the Tasman sea, causing several aviation encounters [*Doiron et al.*, 1991; *Barton et al.*, 1992].

The HIRS/2 retrievals gave very similar results to those obtained from TOMS and because of the greater temporal sampling offer new opportunities to estimate the decay rate of stratospheric SO_2 and permit new studies of the conversion rate of SO_2 to H_2SO_4. Both of these parameters are important to the chemistry of atmospheric SO_2 [*McKeen et al.*, 1984]. Diurnal effects on SO_2 and the relation between SO_2, H_2SO_4 and O_3 (using the HIRS/2 9.7, μm channel) are also possible.

5.3 Ruapehu

The examples given so far can be readily verified against the TOMS data. During 1996 no TOMS instruments were flying and consequently little is known about the SO_2 stratospheric loading during that year. However, there were several volcanic eruptions reported, some of which are likely to have injected SO_2 into the upper troposphere/lower stratosphere.

Between June and August 1996, Mt Ruapehu on the North island of New Zealand erupted several times injecting ash and SO_2 into the atmosphere. Satellite tracking of the Ruapehu plumes using AVHRR data suggested that the ash content of the eruption clouds was significant [*Prata and Grant*, 2001]. Ground-based monitoring of the emissions also suggested that there was significant SO_2 degassing. The first satellite measurements of the SO_2 emissions from Ruapehu are presented here. Results are shown in Plate 3 for retrievals from the NOAA-12 and NOAA-14 HIRS/2 instruments. Maximum SO_2 amounts did not exceed 100 D.U.; the average amounts were ~20–30 D.U. The total mass loadings were less than 0.05 Tg-values of 0.03, 0.02, 0.02, and 0.01 Tg were found for the 17 June, 1996 eruption.

5.4 Hekla–Trajectories

A fourth example of detection and monitoring of relatively small (~< 1 Tg), stratospheric SO_2 clouds from eruptions

Table 4. SO_2 column abundances (Tg) retrieved from HIRS/2 infrared measurements and TOMS ultraviolet measurements [*Bluth et al.,* 1992] for several days after the Pinatubo eruptions of 15 June, 1991. The HIRS/2 means (μ) and standard deviations (σ) are obtained by combining measurements from all three HIRS/2 instruments.

Date	HIRS/2		TOMS
	μ	σ	μ
16-June-1991	15.2	±1.8	15.5
17-June-1991	18.7	±2.2	18.5
18-June-1991	16.5	±1.2	16.0
19-June-1991	15.9	±1.1	14.0
20-June-1991	17.4	±1.1	14.5
21-June-1991	16.3	±0.9	–
22-June-1991	16.9	±1.6	–
23-June-1991	15.0	±1.8	14.0
24-June-1991	12.9	±1.7	–
25-June-1991	11.5	±1.7	–

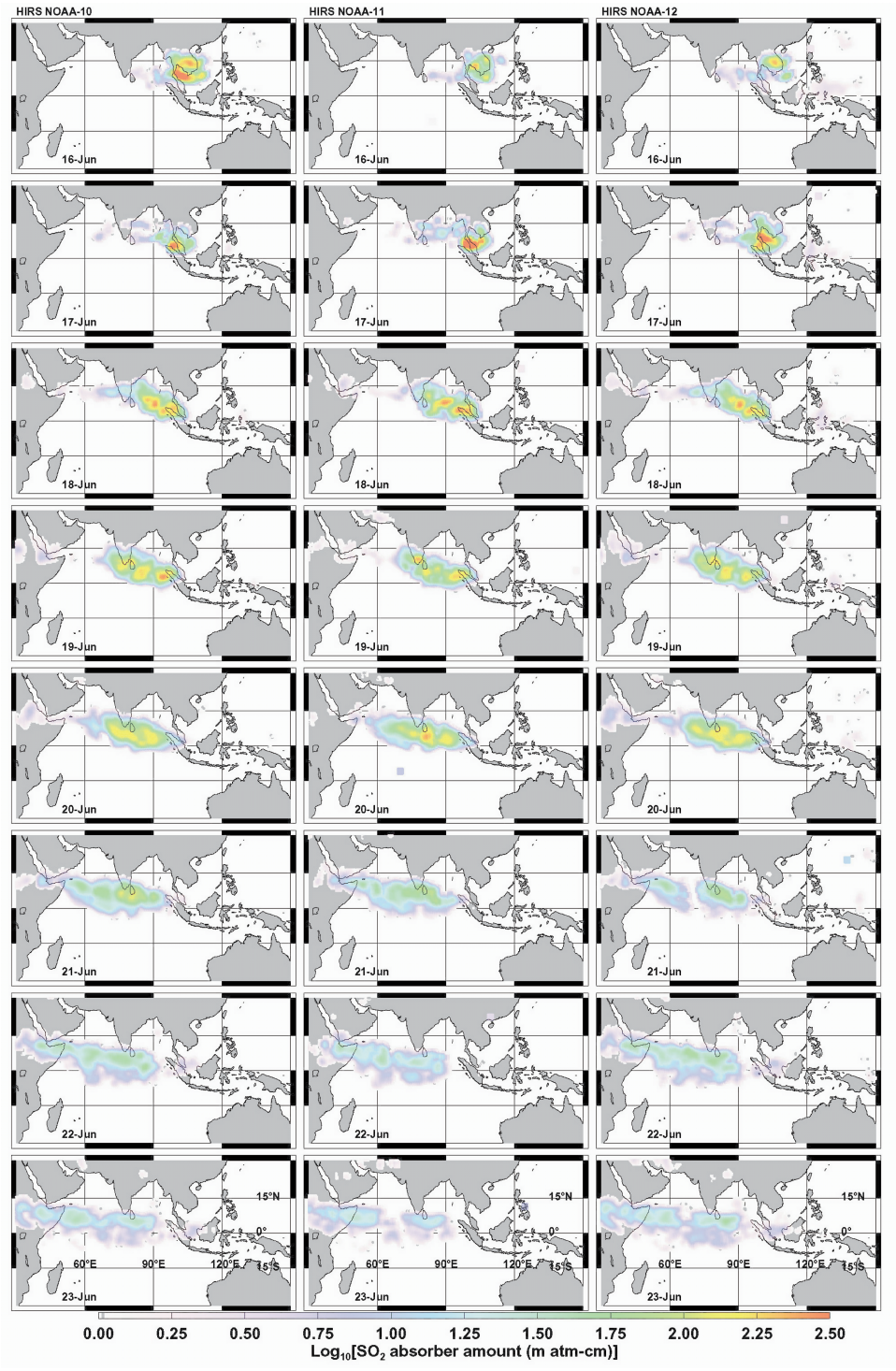

Plate 1. Sequences of SO_2 column abundance (in m atm-cm) from the 15 June, 1991 Pinatubo eruption retrieved from three HIRS/2 instruments.

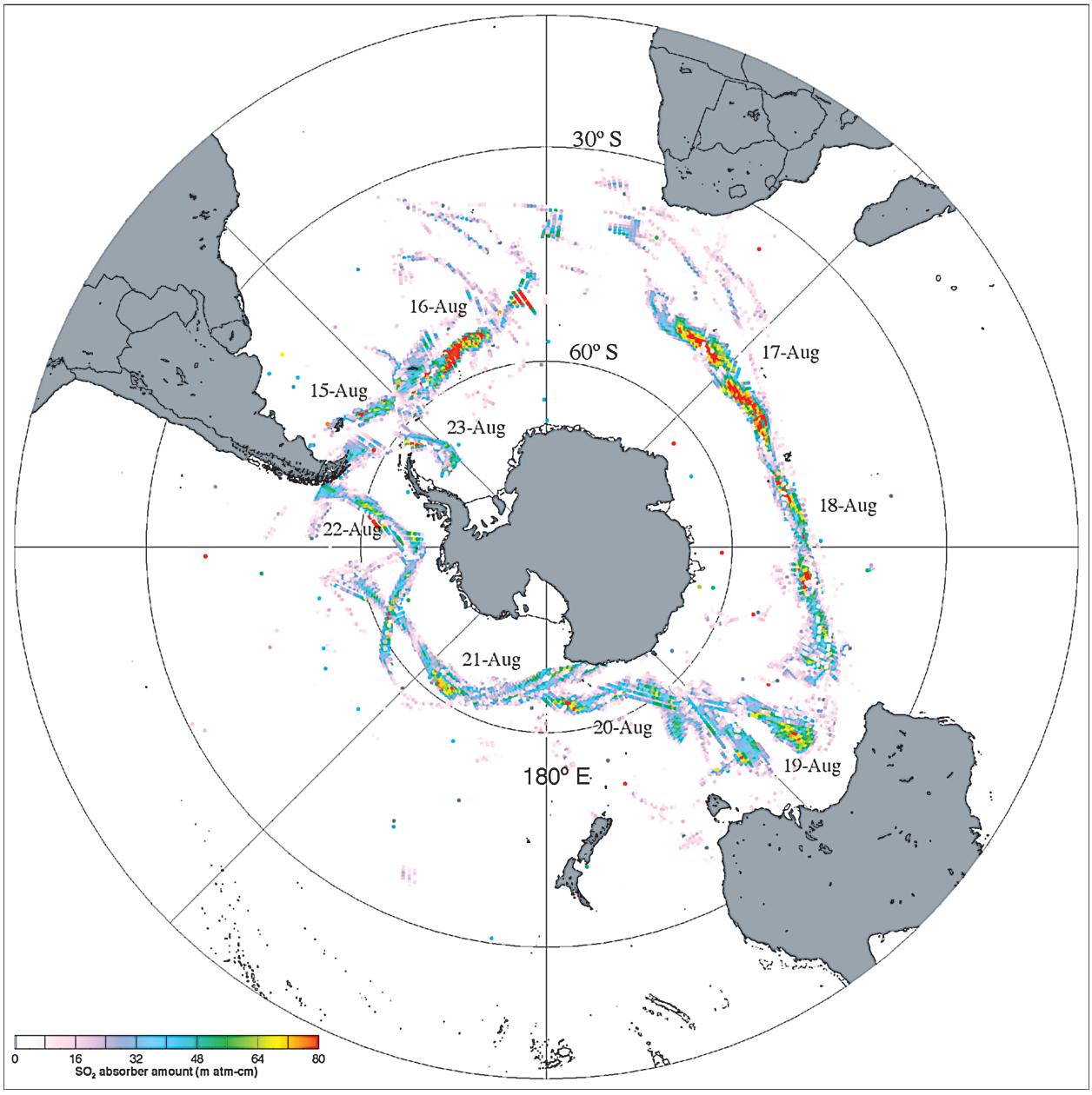

Plate 2. Montage of the SO_2 plume erupted from Cerro Hudson showing how it encircled the southern hemisphere in about 9 days. during August 1991.

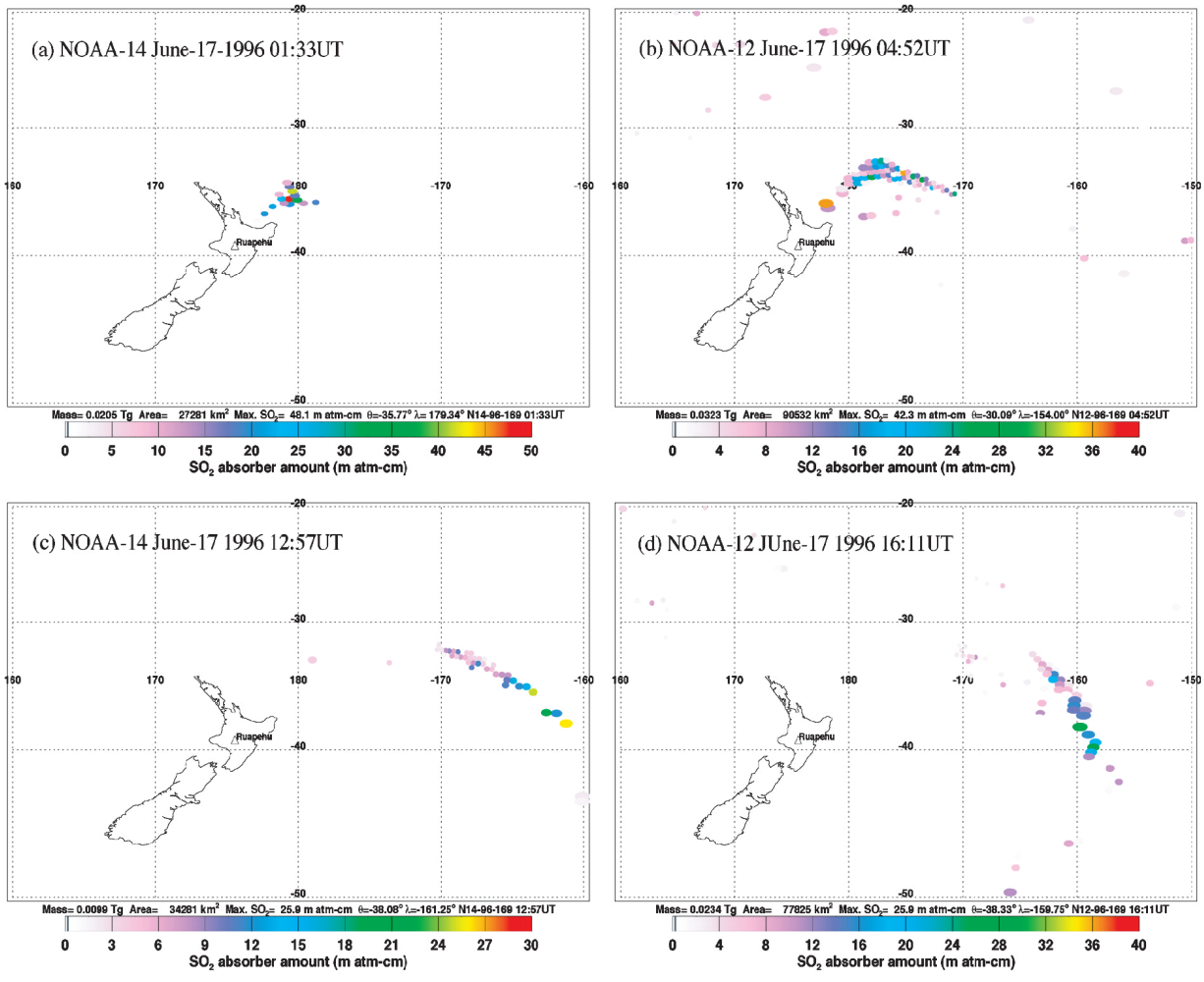

Plate 3. SO_2 retrievals for the 1996 June eruptions of Mt Ruapehu, New Zealand. (a) 01:33UT, 17-June-1996, NOAA-14, (b) 04:52UT, 17-June-1996, NOAA-12, (c) 12:57UT, 17-June-1996, NOAA-14, (d) 16:11UT, 17-June-1996, NOAA-12.

of Hekla volcano, Iceland is provided. These SO_2 clouds typically contain SO_2 amounts of 50 D.U. or less and show that robust detection at the lower limit of detection is possible. We illustrate these retrievals in Figure 5 (a) and Figure 5 (b) by showing the trajectory of the maximum SO_2 amount retrieved during each orbital pass of the satellite. Results are shown for the 1980 and 1991 Hekla eruptions, and demonstrate how these measurements could be used to validate dispersion/trajectory modelling analyses.

5.5 Potential Climate Studies

The importance of sulphur-rich volcanic eruptions to climate has been discussed by *Rampino and Self* [1984]. The

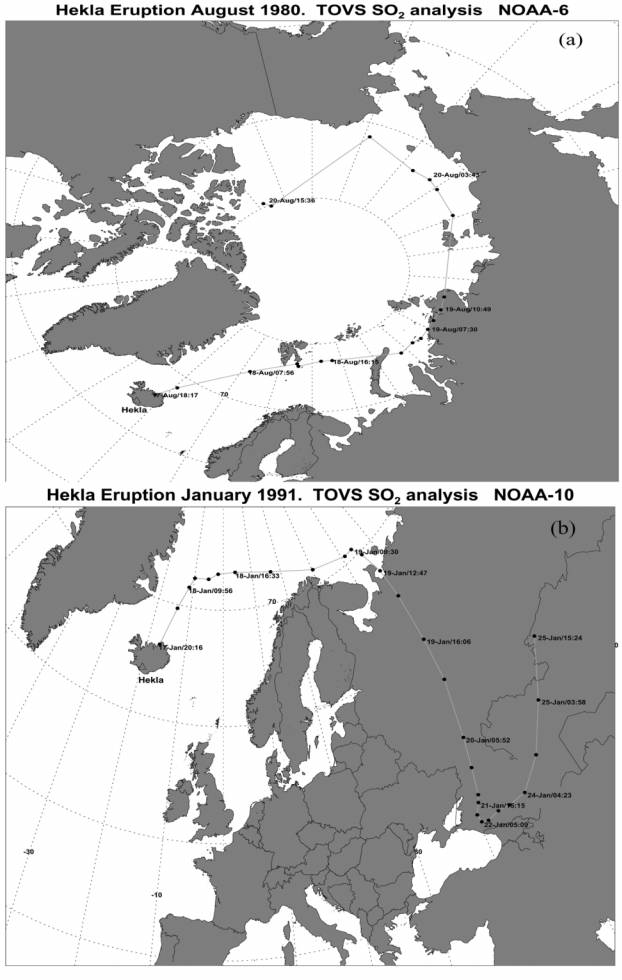

Figure 5. (a) Trajectory of the August 1980 eruption of Hekla, Iceland derived from TOVS HIRS/2 SO_2 retrievals. (b) Trajectory of the January 1991 eruption of Hekla, Iceland derived from TOVS HIRS/2 SO_2 retrievals.

SO_2 retrievals from HIRS/2 are global, have relatively high spatial resolution (up to 18 × 18 km^2 at nadir) and temporal resolution (up to 6 times per day from 3 satellites) and span nearly 24 years. This makes this data set useful for climate studies. To date we have made global SO_2 retrievals for all three HIRS/2 instruments operating during 1991 and have begun analyzing data for other years. The global imprint of SO_2 in the upper troposphere/lower stratosphere during 1991 is shown in Plate 4.

The top panels in the plate show the zonally averaged SO_2 amount, while the lower panels show the zonally integrated SO_2 amount. Intercomparison of the panels provides an estimate of the consistency of the retrievals from two different HIRS/2 instruments. During 1991 there were two climatically significant eruptions: Pinatubo and Cerro Hudson. Pinatubo's SO_2 influence lasted more than 2 months and penetrated well into northern hemisphere midlatitudes. Cerro Hudson's influence was largely restricted to southern hemisphere mid-to-high latitudes and lasted 2–3 weeks. The radiative impact of SO_2 has been studied by *Gerstell et al.* [1995] who recommended that general circulation models should include the radiative forcing due to SO_2 gas as well as H_2SO_4 and volcanic ash. *Pudykiewicz and Dastoor* [1995] simulated the global distribution of sulfate aerosols produced by Pinatubo and found good agreement with aerosol optical depth measurements. These authors introduced the concept of a virtual source–an analytic function that describes the spatial and temporal release of SO_2 into the stratosphere. The analyses presented here could be used as initial conditions for a model that includes the radiative effects of SO_2 and replaces the need for an analytic source function.

6. CONCLUSIONS

The retrieval of SO_2 from HIRS/2 data provides a new global, long-term data set for investigating and quantifying the stratospheric SO_2 budget. These new measurements complement existing TOMS SO_2 data and permit intercomparisons of two independent SO_2 estimates. The HIRS/2 retrieval scheme works best when the SO_2 is separated from water vapour and lies above it–the scheme provides a natural filter for detecting SO_2 that reaches the upper troposphere/lower stratosphere, where its climatic implications are greatest. The error analysis suggests that accuracies are in the range 10–20% for SO_2 column amounts in the range 10–800 m atm-cm. Fundamental difficulties with using infrared measurements prevent making accurate retrievals below and above these limits. Improvements can be made in the retrieval scheme, most notably by using more detailed

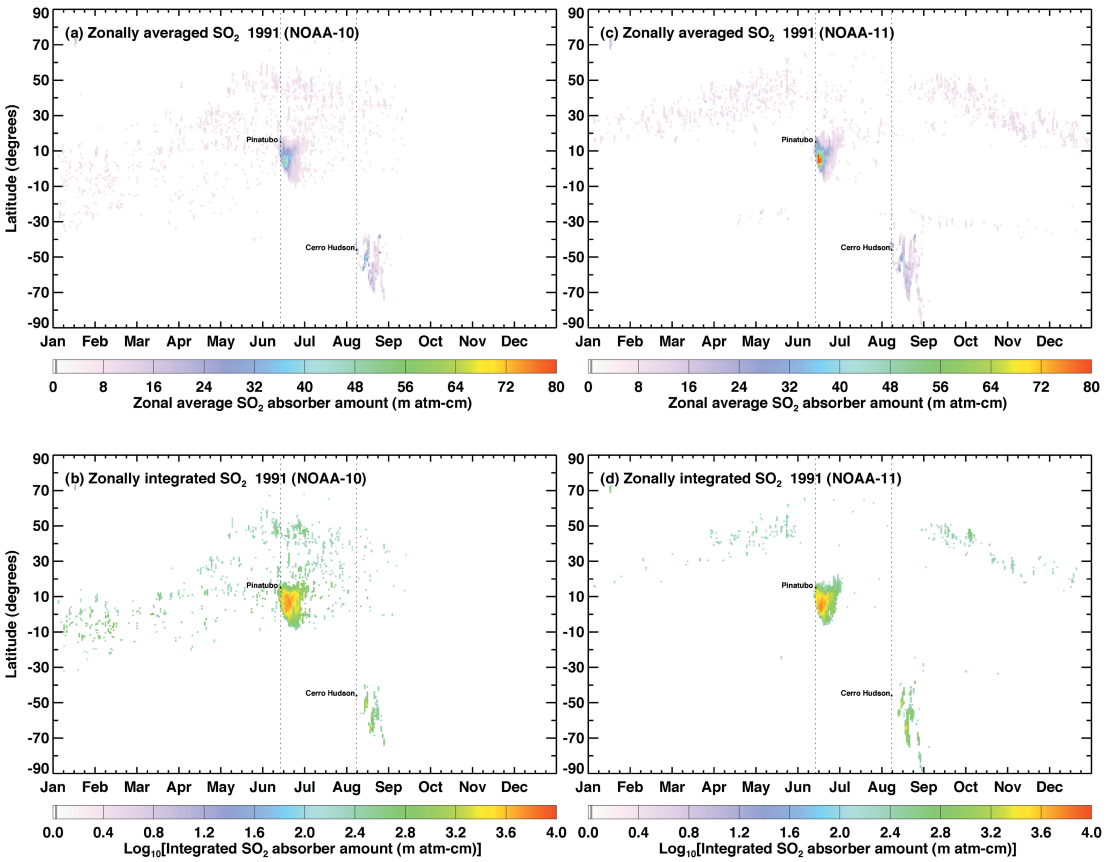

Plate 4. (a) Zonally averaged SO_2 column abundance (m atm-cm) as a function of time and latitude during 1991, derived from the NOAA-10 HIRS/2. (b) Zonally integrated SO_2 column abundance (m atm-cm) as a function of time and latitude during 1991, derived from the NOAA-10 HIRS/2. (c) Zonally averaged SO_2 column abundance (m atm-cm) as a function of time and latitude during 1991, derived from the NOAA-11 HIRS/2. (d) Zonally integrated SO_2 column abundance (m atm-cm) as a function of time and latitude during 1991, derived from the NOAA-11 HIRS/2.

radiative transfer modelling, an improved cloud detection scheme, and better use of the multispectral measurements available with the HIRS/2 instrument. The scheme presented here is fast and ideally suited to operational processing of global data in near real-time.

Further analysis of the HIRS/2 data will permit retrieval of volcanic ash, H_2SO_4 (cf. *Ackerman and Strabala* [1996] and *Baran and Foot* [1994]) as well as SO_2, providing a more comprehensive set of data for understanding the climatic influence of volcanic eruptions. Use of the 9.7 μm HIRS/2 channel in combination with the SO_2 retrievals may also provide new information on the effects of volcanic aerosols on ozone depletion.

The retrieval scheme is not restricted to HIRS/2 data-any instrument with channels near 6.7, 7.3 and 11 μm is amenable to this technique. The MODIS instruments on board Terra and Aqua can be used to derive SO_2 [see Rose et al:, 2003 this volume] as can the new multispectral imager-SEVIRI, on board the Meteosat Second Generation platform. Currently the AIRS instrument on board the Aqua platform can be used to derive SO_2 by exploiting the 7.3 μm feature, with the strong possibility of using the high-spectral content and the narrow channels (up to 2378) to probe the lower troposphere and derive vertical profile information. Perhaps more exciting is the possibility of using the high-spectral resolution data from the Geostationary Infrared Fourier-Transform Spectrometer (GlFTS), which will provide high spatial, temporal and spectral resolution data capable, in principle, of giving SO_2 concentrations at several levels in the upper troposphere/lower stratosphere. To date we have processed only a small part of the considerable global archive of HIRS/2 data. In due course we hope to complete the processing back to the TIROS-N HIRS/2 (1978) and provide a real-time processor for users with access to direct broadcast NOAA data. An operational HIRS/2 SO_2 product would be useful for aviation hazard warning as well as for studying local and global effects of SO_2 on climate.

Acknowledgments. The authors are grateful to Darren Jackson and John Bates both at the NOAA ARL for processing the level la TOVS archive and providing the level lb radiance data. Three anonymous reviewers provided constructive advice on ways to improve this manuscript and we are most grateful to them.

APPENDIX 1: LIST OF ACRONYMS

AIRS–*Atmospheric InfraRed Sounder*
ASTER–*Advanced Spacebourne Thermal Emission and Reflection radiometer*
AVHRR–*Advanced Very High Resolution Radiometer*
HIRS–*High-resolution InfraRed Sounder*
GIFTS–*Geostationary Infrared Fourier-Transform Spectrometer*
GOME–*Global Ozone Monitoring Experiment*
MASTER–*MODIS/ASTER Airborne Simulator*
MODIS–*Moderate-resolution Imaging Spectroradiometer*
NOAA–*National Oceanographic and Atmospheric Administration*
SEVIRI–*Spinning Enhanced Visible amd Infrared Imager*
TIROS–*Television and InfraRed Orbiting Satellite*
TOMS–*Total Ozone Monitoring Spectrometer*
TOVS–*TIROS Operational Vertical Sounder*

APPENDIX 2: RADIATIVE TRANSFER MODEL

The model assumed for analysis of HIRS data has a layer of SO_2 embedded in an otherwise clear atmosphere between heights $z = a$ and $z = b$. Variations in the density of SO_2 and its specific absorption coefficient are assumed to be negligible throughout the layer. The optical thickness from height z to space along a vertical ray is

$$l(z) = \begin{cases} l_a(z) & \text{if } b \le z \\ l_a(z) + \alpha_s (b - z) & \text{if } a \le z \le b \\ l_a(z) + \alpha_s (b - a) & \text{if } z \le a \end{cases}.$$

Here $l_a(z)$ is the optical path from height z to space of an atmosphere without SO_2, and α_s is the volume absorption coefficient of SO_2. The corresponding transmittances from height z to space are

$$t(z) = \begin{cases} t_a(z) & \text{if } b \le z \\ t_a(z) \exp\left(-\alpha_s (b - z)\right) & \text{if } a \le z \le b, \\ t_a(z) \exp\left(-\alpha_s (b - a)\right) & \text{if } z \le a \end{cases}$$

where $t_a(z)$ is the transmittance of an atmosphere without SO_2. We let τ_s and t_s denote the optical thickness and transmittance of the SO_2 column, defined by

$$\tau_s = \alpha_s (b - a) \quad \text{and} \quad t_s = \exp(-\tau_s). \tag{9}$$

The SO_2 layer attenuates the radiance emitted by the atmosphere below, while within the SO_2 layer, where both the atmosphere and SO_2 are active, absorption by each gas modifies the radiance emitted by the other. The radiance I emitted to space consists of four terms,

$$I = t_s I_a + (1 - t_s) I_a^+ + I_{as} + I_{sa}. \tag{10}$$

The first represents the radiance I_a emitted to space by a atmosphere free of SO_2,

$$I_a = B_0 t_a(0) + \int_0^\infty dz\, \alpha_a(z) B(z) t_a(z), \tag{11}$$

attenuated by the transmittance t_s of the SO_2 column. Here α_a (z) is the volume absorption coefficient of the atmosphere at height z, B_0 is the Planck emission by the surface, and $B(z)$ is the Planck emission from the atmosphere at height z where the temperature is $T(z)$. The second term is the radiance I_a^+ emitted by the atmosphere above the SO_2 layer,

$$I_a^+ = \int_b^\infty dz\, \alpha_a(z) B(z) t_a(z), \tag{12}$$

in this case modified by $(1 - t_s)$. The third term represents radiance emitted by the atmosphere within the SO_2 layer and modified there by absorption by SO_2,

$$I_{as} = \int_a^b dz\, \alpha_a B(z) t_a(z) t_s \left[e^{\tau s (z-a)/(b-a)} - 1 \right]. \tag{13}$$

The final term represents radiance emitted by SO_2 and subsequently attenuated by absorption in the atmosphere above the point of emission,

$$I_{sa} = \int_a^b dz\, \alpha_s B(z) t_a(z) e^{-\tau_s (b-z)/(b-a)}. \tag{14}$$

Our analysis of HIRS data is based on two additional assumptions that simplify these equations.

1. We assume that the SO_2 layer lies above the peak of the weighting function for H_2O in the 7.3 μm channel, so that the absorption coefficient α_a (z) is zero for $z > a$. This is a significant assumption, because H_2O absorbs strongly at 7.3 μm and the weighting function peaks relatively high in the atmosphere.
2. The SO_2 layer is assumed to be isothermal, and therefore may be characterized by a single temperature T_s. Clearly, this assumption is questionable when the SO_2 layer is very deep.

Justification for these assumptions is pragmatic, in the sense that the technique appears to track SO_2 plumes from major volcanic eruptions, even though we know that frequently the emission of SO_2 is accompanied by large emissions of H_2O.

With these assumptions, the formulae simplify. Because α_a (z) is zero for $z > a$, the second and third terms in equation (10) are zero, while the fourth term reduces to

$$I_{sa} = \alpha_s B_s \int_a^b dz\, e^{-\tau_s (b-z)/(b-a)} = (1 - t_s) B_s, \tag{15}$$

where B_s denotes the Planck function at the temperature T_s of the SO_2 cloud. Thus,

$$I = t_s I_a + (1 - t_s) B_s, \tag{16}$$

which we also write in the forms

$$I - I_a = (1 - t_s)(B_s - I_a) \text{ and } e^{-\tau_s} = \frac{B_s - I}{B_s - I_a}.$$

Our aim is to estimate τ_s. The data will be observations of the radiance I emitted to space in the HIRS 7.3 μm channel and estimates of B_s and I_a derived from other HIRS/2 channels insensitive to $S0_2$.

NOTES

1. Profiles can also be retrieved but this requires much higher spectral resolution.
2. In keeping with previous practice (e.g. *Krueger et al.* [1995]), we use the units miili atmosphere centimetre (m atm-cm) for absorber amount. 1 m atm-cm =1 D.U. (Dobson Unit) or in S.I. units 1 atm-cm =0.446157 mol m^{-2}
3. An infrared (7.3 μm) optical depth of less than 0.05 is equivalent to ≈2 K difference between the background atmosphere and the SO_2 layer

REFERENCES

Ackerman, S. A., and Strabala, K. I., Satellite remote sensing of H_2SO_4 aerosol using the 8- to 12- μm window region: Application to Mount Pinatubo, *J. Geophys. Res.*, *99*(D9), 18,639-18,649, 1994.

Allard, P., Carbonnelle, J., Métrich, Loyer, H., and Zettwoog, P., Sulphur output and magma degassing budget of Stromboli volcano, *Nature*, *368*, 326-330, 1994.

Baran, A., J. and Foot, J., S., A new application of the operational sounder HIRS in determining a climatology of sulphuric acid aerosol from the Pinatubo eruption, *J. Geophys. Res.*, *99*(D12), 25,673-25,679, 1994.

Barton, I. J., Prata, A. J., Watterson, I. G and Young, S. A., Identification of the Mt. Hudson volcanic cloud over SE Australia, *Geophys. Res. Lett.*, *19*, 1211-1214, 1992.

Berk, A., Bernstein, L. S., and Robertson, D. C., MODTRAN: A moderate resolution model for LOWTRAN 7, U. S., Air Force Phillips Laboratory, Nascom Air Force Base, MA, U. S. A., AFGL-TR-89-0122, 1989.

Bluth, G. J. S., Rose, W. I., Sprod, I. E., and Krueger, A. J., Stratospheric loading of sulfur from explosive volcanic eruptions, *J. Geol. 105*, 671-683, 1997.

Bluth, G. J. S., Schnetzler, C. C., Krueger, A. J., and Walter, L. S., The contribution of explosive volcanism to global atmospheric sulphur dioxide concentrations, *Nature*, *366*, 327-329, 1993.

Chahine, M., Gunson, M., Syvertston, M., and Parkinson, C., AIRS/AMSU/HSB, *NASA Publication*, NP-2001-5-248-GSFC, 21 pp.

Crisp, J., Volcanic SO_2 alert-Version 3, *EOS IDS Volcanology Team Data Product Document-Product #3288*, 13pp, 1995.

Doiron, S. D., Bluth, G. J. S., Schnetzler, C. C., Krueger, A. J., and Walter, L. S., Transport of Cerro Hudson SO_2 clouds, *EOS Trans AGU*, *72*, 489-498, 1991.

Eisinger, M., and Burrows, J. P., Tropospheric sulfur dioxide observed by the ERS-2 DOME instrument, *Geophys. Res. Lett.*, *25*(22), 4177-4180, 1998.

Francis, P., Maciejewski, Oppenheimer, C., Chafes n, C., and Caltabiano, T., SO_2:HCl ratios in the plumes from Mt Etna determined by Fourier transform spectroscopy, *Geophys. Res. Lett.*, *22*(13), 1717-1720, 1995.

Gerstell, M. F, Crisp, J., and Crisp, D., Radiative forcing of the stratosphere by SO_2 gas, silicate ash, and H_2SO_4 aerosols shortly after the 1982 eruptions of El Chichón, *J. Clim.*, *8*, 1060-1070, 1995.

Goldman, A., Murcray, F. J., Rinsland, C. E, Blatherwick, R. D., David, S. J., Murcray, F. H., and Murcray, D. G., Mt Pinatubo SO_2 column measurements from Mauna Loa, *Geophys. Res. Lett.*, *19*(2), 183-186, 1992.

Hofmann, D. J., and Rosen, J. M., On the background stratospheric layer, *J. Atmos. Sci.*, *38*, 168-181, 1981.

Kidwell, K. B., NOAA polar orbiter user's guide-December 1991, *National Oceanic and Atmospheric Administration-NESDIS*, U. S. Department of Commerce, NOAA, Washington D. C., 1991.

Kiehl, J. T., and Briegleb, B. P., The relative roles of sulfate aerosols and greenhouse gases in climate forcing, *Science*, *260*, 311-314, 1983.

Krueger, A. J., Walter, L. S., Bhartia, P. K., Schnetzler, C. C., Kmtkov, N. A., Sprod, I., and Bluth, G. J. S., Volcanic sulphur dioxide measurements from the total ozone mapping spectrometer instruments, *J. Geophys. Res.*, *100*, 14,057-14,076, 1995.

Love, S. P., Goff, F., Counce, D., Siebe, C., and Delgado, H., Passive infrared spectroscopy of the eruption plume at Popocatepétl volcano, *Nature*, *396*, 563-567, 1998.

Mankin, W. G., Coffey, M. T., & Goldman, A., Airborne observations of SO_2, HCl, and O_3, in the stratospheric plume of the Pinatubo volcano in July 1991, *Geophys. Res. Lett.*, *19*(2), 179-182, 1992.

Mass, C. F., and Portman, D. A., Major volcanic eruptions and climate: A critical evaluation, *J. Climate*, *2*, 566-583, 1989.

McCormick, M. P., Thomason, L. W., and Trepte, C. R., Atmospheric effects of the Mt. Pinatubo eruption, *Nature*, *373*, 399-404, 1995.

McGee, K. A., & Gerlach, T. M., Airborne volcanic plume measurements using a FTIR spectrometer, Kilauea volcano, Hawaii, *Geophys. Res. Lett.*, *25* (5), 615-618, 1998.

McKeen, S. A., Liu, S. C., and Kiang, C. S., On the chemistry of stratospheric SO_2 from volcanic eruptions, *J. Geophys. Res.*, *89*(D3), 4873-4881, 1984.

Pierluissi, J. H., and Tomiyama, K., Numerical methods for the generation of empirical and analytical transmittance functions with applications to trace gases, *Appl. Optics*, *19*(14), 2298-2309, 1980.

Pierluissi, J. H., Jarem, J. M., and Maragoudakis, C., Validated transmittance band model for SO_2 in the infrared, *Appl.Optics*, *23*(19), 3325-3330, 1984.

Planet, W. G., Data extraction and calibration of TIROS-N/NOAA radiometers, *NOAA Tech. Rep. NESS 107-Rev. 1*, Natl. Environ. Satell. Data and Inf. Serv., Washington, D.C., 1988.

Prata, A. J., and Grant, I. F, Retrieval of microphysical and morphological properties of volcanic ash plumes from satellite data: Application to Mt Ruapehu, New Zealand, *Quart. J. Roy. Meteorol. Soc.*, *127,* 2153-2179, 2001.

Pndykiewicz, J. A., and Dastoor, A. P., On numerical simulation of the global distribution of sulfate aerosol produced by a large volcanic eruption, *J. Clim.*, *8*, 464-473, 1995.

Pyle, D. M., Beanie, P. D., and Bluth, G. J. S., Sulphur emissions to the stratosphere from explosive volcanic eruptions, *Bull. Volcanol.*, *57*, 663-671, 1996.

Rampino, M. R., and Self, S., Sulphur-rich volcanic eruptions and stratospheric aerosols, *Nature*, *310*, 677-679, 1984.

Randel, D. L., Vonder Haar T. H., Ringerud, M. A., Stephens, G. L., Greenwald, T. J., and C. L. Combs, A new global water vapor dataset, *Bull. Amer. Meteorol. Soc.*, *77*(6), 1233-1246, 1996.

Realmuto, V. J., Abrams, M. J., Buongiorno, M. F., and Pieri, D. C., The use multispectral thermal infrared image data to estimate sulfur dioxide fhx from volcanoes: A case study from Mount Etna, Sicily, July 29, 1986, *J. Geophys. Res.*, *99*, 481-488, 1994.

Realmuto, V. J., Volcanic SO_2—High and moderate spatial resolution, Version 3, *EOS IDS Volcanology Team Data Product Document-Product #3289*, 20pp, 1995.

Robock, A., Volcanic eruptions and climate, *Rev. Geophys.*, *38*(2), 191-219, 2000.

Rose, W. I., Bluth, G. J. S., and Ernst, G. G. J., Integrating retrievals of volcanic cloud characteristics from satellite remote sensors: a summary, *Phil. Trans. R. Soc. London A.*, *358*, 1585-1606, 2000.

Rose, W. I., Gu, Y., Watson, I. M., Yu, T., Bluth, G. J. S., Prata, A. J., Krueger, A. J., Krotkov, N., Carn, S., Fromm, M. D., Hunton, D., Viggiano, A. A., Miller, T. M., Ballentin, J. 0., Ernst, G. G. J., Reeves, J. M., Wilson, C., and Anderson, B. E., The February-March 2000 eruption of Hekla, Iceland from a satellite perspective, *This volume*, 2003.

Self, S., Zhao, J-X, Holasek, R. E., Torres, R. C., and King, A. J., The atmospheric impact of the 1991 Mount Pinatubo eruption, *In Fire and Mud: Eruptions and Lahars of Mount Pinatubo, Philippines, C. G. Newhall and R. S. Punongbayan, eds., Philippine Institute of Volcanology and Seismology, Queen City, and University of Washington Press, Seattle*, 1089-1115, 1996.

Seinfeld, J. H., and Pandis, S. N., Atmospheric chemistry and physics. From air pollution to climate change. *John Wiley and Sons, New York*, 1326 pp, 1998.

Smith, W. L., Woolf, H. M, Hayden, C. M., Wark, D., and McMillin, L. M., The TIROS-N operational vertical sounder, *Bull. Amer. Meteorol. Soc.*, *60*, 1177-1187, 1979.

Stoiber, R., and Jepsen, A., Sulfur dioxide contributions to the atmosphere by volcanoes, *Science*, *182*, 577-578, 1973.

Wiscombe, W. J., and Evans, J. W., Exponential-sum fitting of radiative transmission functions, *J. Comp. Phys.*, *24*, 416-444, 1977.

D. M. O'Brien, CSIRO Atmospheric Research, PB1, Aspendale, Victoria 3195, Australia, Email: Denis.O'Brien@csiro.au

A. J. Prata, CSIRO Atmospheric Research, PB1, Aspendale, Victoria 3195, Australia, Email: Fred.Prata@csiro.au

W. I. Rose, Geological Engineering and Sciences, Michigan Technological University, Houghton, Michigan, USA, Email: raman@mtu.edu

S. Self, Department of Earth Sciences, The Open University, Walton Hall, Milton Keynes, MK7 6 AASA, United Kingdom, Email:Stephen.Self@open.ac.uk.